

# Impulse Noise Modeling in an Indoor Narrowband Power Line Communication Channel using M-QAM and a Software-Defined Radio Approach

Akintunde Oluremi, Iyiola\*, Ayokunle Damilola, Familua†, Thokozani, Shongwe\*, and Theo G. Swart†

\*Department of Electrical and Electronics Engineering Technology, University of Johannesburg,  
P.O. Box 17011, Doornfontein, 2028, Johannesburg, South Africa

†Department of Electrical and Electronics Engineering Science, University of Johannesburg,  
P.O. Box 524, Auckland Park, 2006, Johannesburg, South Africa

Email: 218032385@student.uj.ac.za, familuaad@uj.ac.za, tshongwe@uj.ac.za, tgswart@uj.ac.za

**Abstract—**Noise is generated on the indoor Narrowband Power Line Communication channel by the uncoordinated activities of several electrical devices connected to the power line networks, and by radiated environmental disturbances. There is a need to overcome these noise and channel impairments for reliable communication to be achieved. Statistical channel modeling of noise will facilitate the development and optimization of dependable PLC systems. Thus, in this work, we have developed a Software-Defined-PLC transceiver and test-bed that adopts 4, 8 and 16 Quadrature amplitude modulation schemes and uses the Universal Software Radio Peripheral and MATLAB/Simulink platforms to facilitate impulsive noise error measurement and modeling using the three-state Fritchman Markov Model (FMM) and the Baum-Welch Algorithm. The statistical channel models obtained are accurate derived channel models based on experimental measurement. The close match between the experimental and model error-free run distribution and error probabilities justify the modeling of the PLC memory channel using the three-state FMM. The model results obtained will assist in the implementation of error correction systems and novel optimization techniques in an impulsive noise PLC channel environment.

**Index Terms—**Baum-Welch Algorithm (BWA), Fritchman Markov model, Quadrature Amplitude Modulation (QAM), Narrowband Power Line Communication (NB-PLC), Universal Software Radio Peripheral (USRP).

## I. INTRODUCTION

Power Line Communication (PLC) has gained tremendous attention in recent years for data transmission and indoor networking, as electrical power outlets are widely accessible in almost every home and office across the globe. Intensive PLC research and development over the last decades has led to the development of standards and regulations for PLC. Therefore, the existing PLC systems based on the classification of frequency bands have been described in [1] and divided into Broadband PLC (BB-PLC) and Narrowband PLC (NB-PLC). The NB-PLC can be adopted for smart metering, smart home, and street lighting in residential and industrial areas [2].

This work is based on research supported in part by the National Research Foundation of South Africa (UID 118693).

The NB-PLC channel is among the most challenging communication channels because the channel itself was designed for the supply of electricity to end user devices, not for communication purposes. Consequently, the uncoordinated use of many connected electronic devices has created high-amplitude impulsive noise [3], which causes burst errors, corrupts transmitted information and impedes efficient transmission and reception of information signals. Specifically, studies of various noise measurement campaigns in PLC environments have shown that PLC noise is non-Gaussian, impulsive and correlated [4], [5]. Therefore, noise measurement campaigns to achieve accurate PLC channel models are crucial for achieving reliable communication and for mitigating the degradation of data signals resulting from the impact of impulse noise in the indoor PLC environment.

In PLC noise modeling, the first major problem that needs to be addressed is the development of accurate and appropriate models that depict PLC noise characteristics including impulsive memory, and that can facilitate the development of novel PLC systems design and evaluation. Numerous methods have been proposed and used in literature to model memory channels, such as impulsive noise PLC channels [6]–[8]. However, Fritchman Markov Models (FMMs) are the most commonly used functional methods for modeling memory channels to generate approximate statistical models for the channel being considered. FMM was used for a range of communication applications, such as wireless networks [9], visible light communication [10] and PLC [11], [12].

The starting point for PLC channel modeling is the use of a transceiver system test-bed to obtain the experimental-based measurements in a controlled PLC environment. There are essentially two types of transceiver measurement systems used for the PLC measurement campaign: re-programmable transceivers [12] and non-programmable transceiver systems [13]. For this study, a re-configurable software defined radio (SDR) platform was used to develop a reliable transceiver and test-bed that helps test the functionality of the system and properly assesses the

performance of modulation schemes and forward error correction (FEC) techniques.

In January 2010, the ITU-T launched the G.HNEM [14] project with the aim of establishing a unified standard for integration between G3-PLC and PRIME [15], two NB-PLC standards. They suggested QAM as the OFDM element in their specification. Based on this, we have selected M-ary QAM in our work. Therefore, our contributions in this study are threefold. Firstly, to design and implement an uncoded M-QAM (4-QAM, 8-QAM, and 16-QAM) based Software-Defined PLC (SD-PLC) transceiver system using USRP hardware and MATLAB/Simulink software platform to obtain a reliable transceiver system and test-bed for measuring and modeling impulsive noise errors in a NB-PLC system operating in the CENELEC-C frequency band. Secondly, to conduct real-time data transmission for the different M-QAM schemes using the developed SD-PLC experimental test bed, integrating various interconnected indoor electrical devices that serve as impulse noise sources on the network and obtain experimental data (error sequences). Finally, to investigate the suitability of applying FMMs and Baum-Welch algorithm (BWA) to the indoor NB-PLC channel for modeling impulse noise errors.

The rest of this work is presented thus: Section II describes the SD-PLC transceiver system model, Section III discusses the Fritchman Markov Model adopted in this study, and Section IV presents the experimental set-up and measurements results. Section V presents the modeling results and analysis. Finally, Section VI provides the concluding remarks.

## II. SD-PLC TRANSCEIVER SYSTEM MODEL

This work involves the development of SD-PLC transceiver systems for real-time data transmission, error sequence measurement and NB-PLC channel modeling using re-programmable USRP hardware and QAM modulation techniques. The USRP hardware is a fully programmable, modular and efficient SDR transceiver manufactured by Ettus Research, a subsidiary of National Instruments [16]. The integration of USRP transceiver modules, PLC coupling circuits (bandpass filters), software platforms and personal computers (PCs) enables the prototyping of PLC systems.

In this work, we used the Ethernet-based USRP N210 with the LFTX transmitter daughterboard and the LFRX receiver daughterboard combined with the Power Line Coupling interface as our hardware platform and our programming language was MATLAB/Simulink for real-time signal transmission and reception. The coupling interfaces are the most important part of the SD-PLC transceiver system. Thus, appropriate transmission and receiving coupling interfaces must be selected or developed to transmit and receive on the indoor NB-PLC channel. For this study, the STEVAL-XPLM01CPL coupling circuit designed by ST Microelectronics, which was purchased off the shelf was used.

Fig. 1 shows the SD-PLC QAM transceiver system model considered in this study. The system performs several complex operations simultaneously to enable efficient data transmission and reception. On the transmitter side, the data

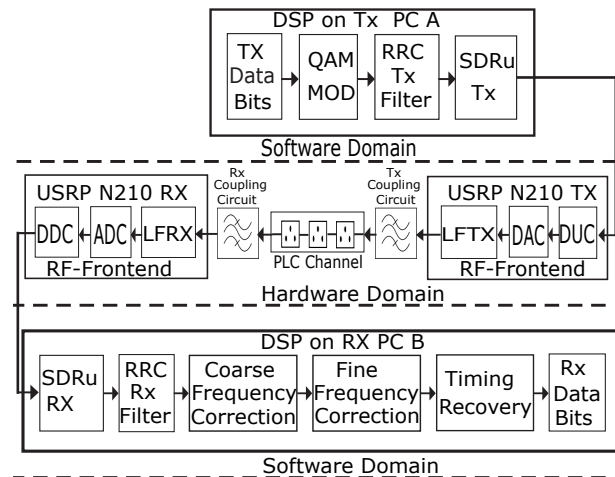


Fig. 1. The SD-PLC QAM transceiver system

bits are first mapped using the QAM (4-QAM, 8-QAM, 16-QAM) modulator to obtain the modulated baseband signal on the host Transmitter (Tx) PC. After that, the pre-processed modulated signal from the host Tx PC, through the SDRu Transmitter Simulink block, reaches the USRP transmitter via the gigabit Ethernet data port. The samples are then interpolated, which involves an increase in the sampling rate and filtering prior to digital up-conversion (DUC) [17]. The Tx USRP FPGA then performs DUC after interpolation by converting the digital complex signal from baseband to digital passband equivalent. Subsequently, the USRP-FPGA processed digital passband signal is translated into an analog equivalent signal by the digital-to-analog converter (DAC) and forwarded to the LFTX-daughterboard for further modification. The LFTX-daughterboard then modulates the Tx streams from intermediate frequency (IF) to the CENELEC-C band operational-frequency. The continuous analog output signal is now transmitted and superposed on the voltage signal of the power line channel through the transmitter coupling interface.

On the receiver end of the system, the processing tasks involve the reception, synchronization, and demodulation of the transmitted QAM signal. First, the receiver (Rx) coupling interface decouples the transmitted QAM signal from the power line channel to the Rx USRP via the LFRX-daughterboard. Subsequently, the USRP LFRX-daughterboard then filters and modulates the analog signal obtained, initially sampling them from the CENELEC-C band transmit-frequency to intermediate frequency (IF), and then multiplies them by discrete complex samples. The analog signal obtained is converted to the digital baseband form by the analog-to-digital converter (ADC) for further processing of the baseband signal. The digital down-converter (DDC) then filters and decimates the resulting digital baseband bit stream, removing dual-frequency components and reducing the sample rate. Subsequently, the resulting digital samples are eventually placed in the buffer and transmitted to the host Rx computer through the gigabit Ethernet port for further post-processing of the baseband signal. Finally, the QAM signal demodulator along with

the SDRu receiver demodulates the baseband signals and the initially transmitted signal is recovered correctly in the absence of channel or noise disturbance.

### III. THE FRITCHMAN MARKOV MODELS

The Fritchman Markov Model, a probabilistic model that statistically describes burst error occurrences in a discrete communication channel, was originally proposed by Fritchman [18] in 1967. It uses discrete-time finite-state Markov models to describe channel conditions and is described in telecommunications literature as a type of Semi-Hidden Markov Model (SHMM) [19]. Fritchman's framework partitions the process of data transmission into two states:  $g$  good states and  $N - g$  bad states. A correctly received bit (error-free) describes a good state, while a bad state is defined by an incorrectly received bit (error) in transmission. A good state is characterized by accurate transmission without error, marked with '0' whereas a bad state is often described and identified with a transmission error denoted by '1'. An FMM with a single-error state was successfully used for modeling an indoor PLC channel in [20], visible light communication channel in [10] and underwater acoustic channel in [21]. In every case, the channel burst behavior was conveniently represented by two or three good states (error-free) at a reasonable degree of accuracy. Accordingly, as illustrated in Fig. 2, this study

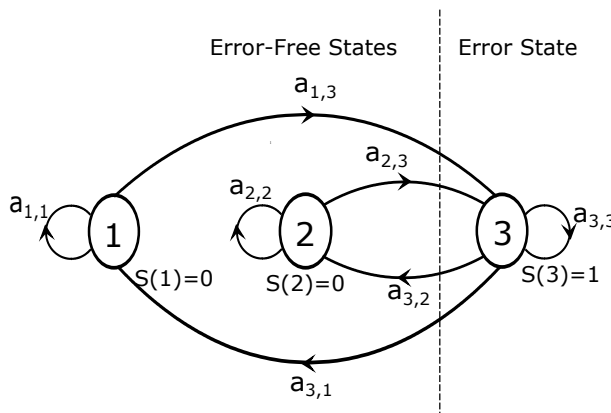


Fig. 2. Three-State FMM Model

adopted a three-state FMM model, which has two good states and a bad state. Fig. 2 shows that transitions between states of the same group are not permitted for the three-state FMM. This means different degrees of memory are available; therefore, it is possible to model a real communication channel. For the three-state FMM adopted in this work, the state transition probability matrix representation and initial values adopted for modeling is denoted by  $A$  as:

$$A = \begin{bmatrix} a_{11} & 0 & a_{13} \\ 0 & a_{22} & a_{23} \\ a_{31} & a_{32} & a_{33} \end{bmatrix} = \begin{bmatrix} 0.8 & 0 & 0.20 \\ 0 & 0.70 & 0.30 \\ 0.10 & 0.70 & 0.20 \end{bmatrix} \quad (1)$$

For the above  $A$  matrix, transitions between good states are not possible, which makes the elements  $a_{12}$  and  $a_{21}$  zeros. The error generation matrix  $B$  is another model parameter that describes the probability that an error will be generated

at a discrete time in a particular state. In view of the fact that good states are error-free and that errors are always generated in bad states, the error generation matrix for three-state FMM models is specified accordingly as:

$$B = \begin{bmatrix} 1 & 1 & 0 \\ 0 & 0 & 1 \end{bmatrix} \quad (2)$$

If an error occurs, it can be observed that the error was generated by state 3, but if no error is generated, it can not be observed which of the good states created the correctly received bits, this explains why the model is labeled a semi-hidden Markov model.

The initial or prior probability of being in any state at a discrete-time is the last parameter of the model as shown:

$$\pi = [\pi_1 \ \pi_2 \ \pi_3] = [0.4 \ 0.4 \ 0.2] \quad (3)$$

The full parameter set for the adopted three-state FMM model is denoted by  $\Gamma = (A, B, \pi)$ .

#### A. Baum-Welch Algorithm

The BWA is a robust technique for evaluating the FMM parameters. It is an iterative algorithm and dynamic programming method used to estimate the full parameter set  $\Gamma = (A, B, \pi)$  that depicts the measured or simulated errors sequence [19]. The experimentally measured error sequences and the initialized FMM parameters are the training and input data for the algorithm. The algorithm concentrates on adjusting the complete set of initialized FMM parameters  $\Gamma = (A, B, \pi)$  to achieve the most likely set of parameters representing the measured error sequences. It employs the maximum likelihood estimation method to estimate the parameters of the model. Refer to Appendix A in [12] for a detailed mathematical representation of the BWA.

### IV. EXPERIMENTAL SETUP

The experimental test-bed was set up at the University of Johannesburg, Auckland Park Communications Laboratory, with careful consideration given to achieving best configuration for the measurement of error sequences.

Fig. 3 shows the architecture of the experimental setup, while in Fig. 4 the photograph of the setup is shown. As shown in Fig. 3, the following are the constituent

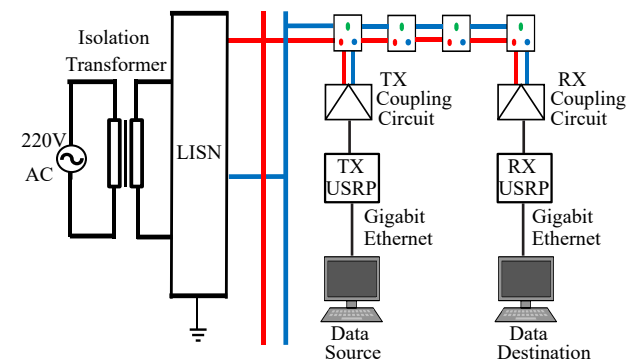


Fig. 3. The experimental test-bed schematics

elements of the PLC measurement test-bed: the isolation transformer, line impedance stabilization network (LISN), power line topology, transmitting and receiving coupling

circuits, transmitting and receiving USRP, transmitting host and receiving host PCs. The impedance of the network is not constant in power line networks, which varies with the mains voltage. This variation causes a mismatch of impedance between measuring equipment and line. This condition needs to be eliminated to improve the efficiency of the outcomes of the measurements. A LISN is used to address this problem as well as to isolate the system from the mains voltage.



Fig. 4. A photograph of the experimental test-bed

TABLE I  
HARDWARE & SOFTWARE CONFIGURATION

ITEMS	VALUES & CONFIGURATIONS
USRP Hardware (TX and RX)	USRP N210
TX daughterboard model	LFTX, (0-30MHz)
RX daughterboard model	LFRX, (0-50MHz)
TX Computer/USRP TX IP	192.168.20.1 & 192.168.20.2
RX Computer/USRP RX IP	192.168.40.1 & 192.168.40.2
Constellation order	4, 8, 16 QAM
Transmitter & Receiver gain	non-tunable (default)
USRP FPGA & Firmware rev	003.005.003
CENELEC-C frequency	130kHz
Sample time	6μs
Sample frequency	200kHz
Tx & Rx bit length	50,000
Host PC TX & RX OS	Windows 10 Pro, 64 bits
Host PC TX & RX Processor	Intel(®) Core(TM) i5-4300u
Host-based Software Version	Matlab R2017a(9.2.0.538062)

The essential software, hardware, and transmission configuration parameters used in our implementation are included in Table I. In this study, the effects of uncoordinated switching ON and OFF of a compact fluorescent lamp (CFL) bulb and hair dryer on the transmitted digital data over the indoor SD-PLC system are measured. Hence, the use of the CFL-bulb and hairdryer as impulsive noise generator helps to obtain the statistical error distribution in the indoor NB-PLC channel due to the impulse noise effects.

## V. RESULTS AND ANALYSIS

The error sequence was generated by comparing sent and received bits. “0” indicates the receiver receiving the right bit, while “1” corresponds to the reception of wrong bits. The transmitted bits, received bits, and the measured error sequence length is 50,000. The error bit positions of device

1 (CFL-bulbs under 16-QAM system) and device 2 (hairdryer under 16-QAM system) are shown in Figs. 5 and 6. The long burst error is severe in the 16-QAM system in both cases as can be deduced from the figures. This is because higher-order QAM can transmit more data as a result of higher bandwidth compared to low-order QAM, but because of its high error rate, it is less efficient compared to lower-order QAM.

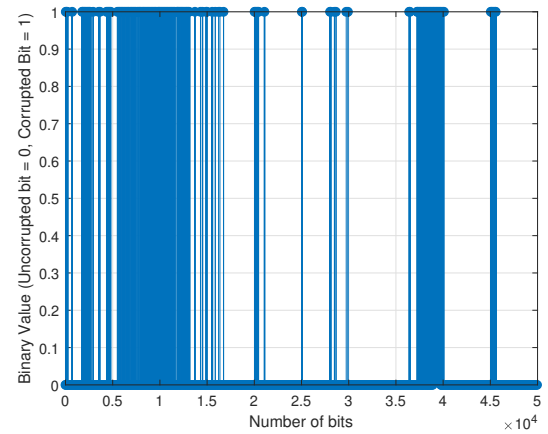


Fig. 5. Error Sequence for 16-QAM (with CFL-bulb)

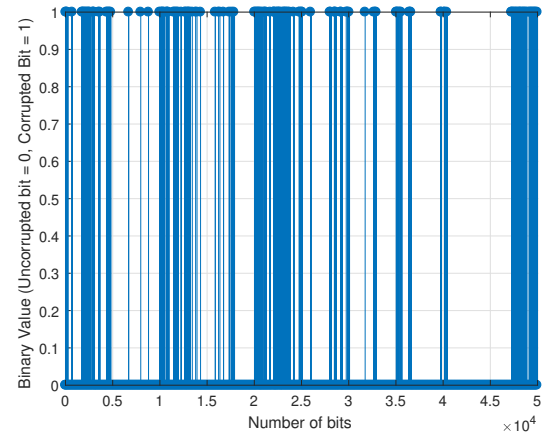


Fig. 6. Error Sequence for 16-QAM (with hair dryer)

The error sequence obtained experimentally was the training data to the BWA, while the FMM parameters were initialized and then became an input for the BWA. The resulting model parameters are the most probable parameters for each of the QAM schemes that have produced the corresponding measured error sequence, given the initialized model parameters  $\Gamma = (A, B, \pi)$ .

### A. Estimated State Transition Probabilities

The estimated state transition probabilities represents the model, and depicts the most probable model parameters that produced the measured error sequences. Tables II and III show the most probable estimated state transition probabilities that depict the measured error sequences for case 1 (with CFL-bulb) and case 2 (with hair dryer) respectively.

TABLE II  
ESTIMATED STATE TRANSITION PROBABILITIES FOR CASE 1  
(CFL-BULB)

A	4-QAM	8-QAM	16-QAM
$a_{11}$	0.9918	0.9903	0.9902
$a_{13}$	0.0082	0.0097	0.0098
$a_{22}$	0.9528	0.9768	0.9579
$a_{23}$	0.0472	0.0232	0.0421
$a_{31}$	0.0694	0.0145	0.0089
$a_{32}$	0.5923	0.5347	0.4506
$a_{33}$	0.3383	0.4508	0.5405

TABLE III  
ESTIMATED STATE TRANSITION PROBABILITIES FOR CASE 2 (HAIR DRYER)

A	4-QAM	8-QAM	16-QAM
$a_{11}$	0.9916	0.9904	0.9920
$a_{13}$	0.0084	0.0096	0.0080
$a_{22}$	0.9316	0.9467	0.9475
$a_{23}$	0.0684	0.0533	0.0525
$a_{31}$	0.0304	0.0049	0.0275
$a_{32}$	0.6164	0.5054	0.4050
$a_{33}$	0.3532	0.4897	0.5675

The non-uniform estimated state transition probability distribution observed from both Tables II and III is due to non-identical measured error sequences obtained, with the high-order QAM having higher error probability when compared to low error probability recorded for the low-order QAM scheme.

### B. Log-likelihood Ratio Plots

The log-likelihood ratio (LLR) is utilized in measuring the accuracy of a statistical model to a data sample.

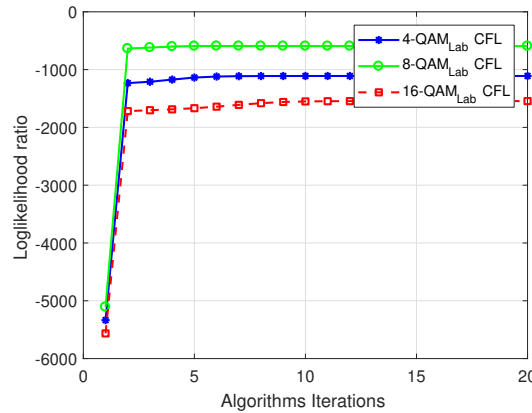


Fig. 7. LLR plot for Case 1 (CFL-bulb)

The BWA converges to a maximum likelihood estimate [19]. Convergence is reached at the second iteration, with the desired degree of convergence to four decimal places achieved at the twentieth iteration as seen in Figs. 7 and 8, at which point the estimated state transition probability values do not change.

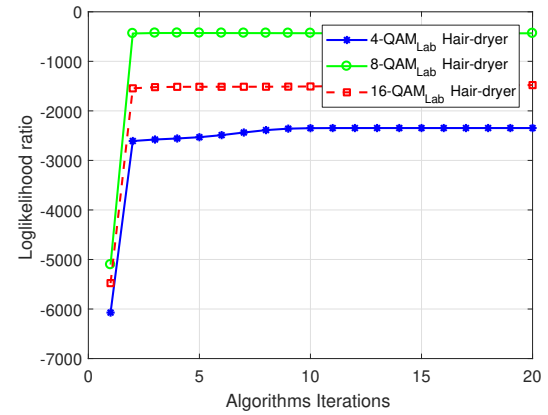


Fig. 8. LLR plot for Case 2 (hair dryer)

### C. Error-free Run Distribution Graphs

The error-free run distribution (EFRD) graph shows the probability of crossing over to  $m$ -consecutive error-free transmissions after an error transmission.

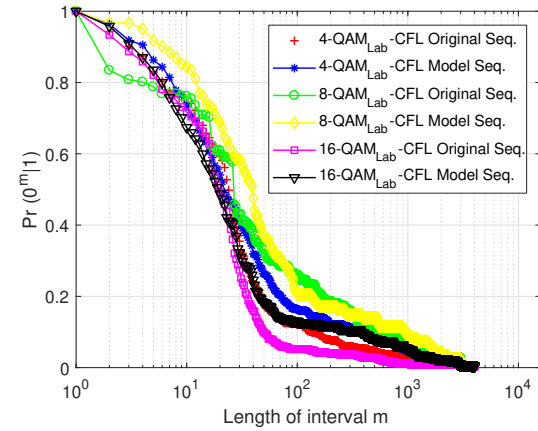


Fig. 9. EFRD graph for Case 1 (CFL-bulb)

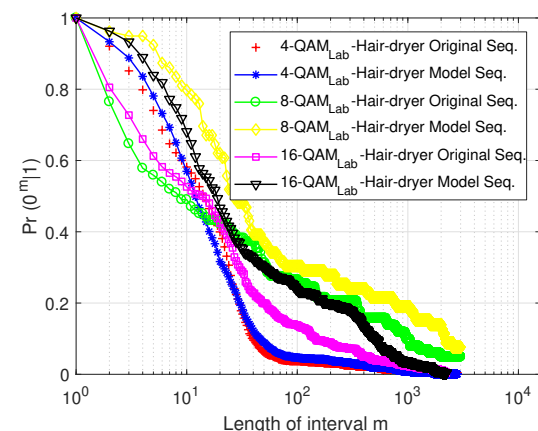


Fig. 10. EFRD graph for Case 2 (hair dryer)

An estimate of the burst or clustering of bit errors is provided through the distribution of error-free runs. Figs. 9 and 10 depict the EFRD graph, which is denoted by  $Pr(0^m|1)$  for both cases under investigation. An examination of Figs.

9 and 10 show a close agreement between the EFRD of the experimentally obtained error sequence and EFRD of the FMM generated error sequences, which confirms that the estimated FMM is accurate and reliable.

#### D. Error Probabilities

The probabilities of error is another metric used to determine the accuracy of the FMM and to assess the accuracy of the estimated model. Tables IV and V show the probabilities of error for the experimental error sequences and the FMM generated error sequences for case 1 and case 2.

TABLE IV  
PROBABILITIES OF ERROR FOR MEASURED ERROR SEQUENCES ( $P_o$ )  
AND FMM GENERATED ERROR SEQUENCES ( $P_m$ ) FOR CASE 1  
(CFL-BULB)

	<b>4-QAM</b>	<b>8-QAM</b>	<b>16-QAM</b>
$P_o$	0.0166	0.0338	0.0515
$P_m$	0.0144	0.0362	0.0536

TABLE V  
PROBABILITIES OF ERROR FOR MEASURED ERROR SEQUENCES ( $P_o$ )  
AND FMM GENERATED ERROR SEQUENCES ( $P_m$ ) FOR CASE 2 (HAIR  
DRYER)

	<b>4-QAM</b>	<b>8-QAM</b>	<b>16-QAM</b>
$P_o$	0.0323	0.0526	0.0597
$P_m$	0.0338	0.0568	0.0552

The relative consistency between  $P_o$  for the experimental error sequences and  $P_m$  for the FMM generated error sequences confirms the precision of the estimated model.

## VI. CONCLUSION

In this study, we reported the development of an uncoded M-QAM SD-PLC transceiver using USRP hardware and DSP algorithms to achieve a versatile NB-PLC transceiver and test-bed for experimental impulsive noise error measurement and subsequently obtained channel error statistics for channel modeling. Error statistics were obtained by comparing transmitted and received bits in the presence of impulse noise sources. Following a series of successful experimental measurements, long burst errors were minimal in 4-QAM and 8-QAM and severe in 16-QAM in both cases. Since higher-order QAM can transmit more data due to higher bandwidth than low-order QAM, its high error rate makes it less effective than lower-order QAM. For modeling of an indoor NB-PLC channel, a three-state FMM was adopted, and reliable channel models based on experimental measurements were obtained. The close agreement between experimental and model-generated EFRDs and probabilities of error confirms that the FMM is suitable for modeling of memory PLC channels. Therefore, these results can be exploited to improve modulation schemes' efficiency, improve and optimize NB-PLC systems and develop error-correction techniques to reduce noise impacts on the NB-PLC channel for Smart Home applications.

## REFERENCES

- [1] S. Galli, A. Scaglione, and Z. Wang, "For the grid and through the grid: The role of power line communications in the smart grid," *Proceedings of the IEEE*, vol. 99, no. 6, pp. 998–1027, 2011.
- [2] H. C. Ferreira, L. Lampe, J. Newbury, and T. G. Swart, *Power Line Communications: Theory and Applications for Narrowband and Broadband Communications over Power Lines*. John Wiley & Sons, 2011.
- [3] S. Güzelgöz, H. B. Çelebi, T. Güzel, H. Arslan, and M. K. Mihçak, "Time frequency analysis of noise generated by electrical loads in PLC," in *17th International Conference on Telecommunications*, 2010, pp. 864–871.
- [4] D. Fertonani and G. Colavolpe, "On reliable communications over channels impaired by bursty impulse noise," *IEEE Transactions on Communications*, vol. 57, no. 7, pp. 2024–2030, 2009.
- [5] M. Zimmermann and K. Dostert, "Analysis and modeling of impulsive noise in broad-band powerline communications," *IEEE Transactions on Electromagnetic Compatibility*, vol. 44, no. 1, pp. 249–258, 2002.
- [6] L. N. Kanal and A. Sastry, "Models for channels with memory and their applications to error control," *Proceedings of the IEEE*, vol. 66, no. 7, pp. 724–744, 1978.
- [7] D. Umebara, S. Hirata, S. Denno, and Y. Morihiro, "Modeling of impulse noise for indoor broadband power line communications," *Proc. International Symposium on Information Theory and Its Applications*, pp. 195–200, 2006.
- [8] P. Sadeghi, R. A. Kennedy, P. B. Rapajic, and R. Shams, "Finite-state Markov modeling of fading channels —a survey of principles and applications," *IEEE Signal Processing Magazine*, vol. 25, no. 5, pp. 57–80, 2008.
- [9] S. Kordnoori, H. Mostafaei, and M. Behzadi, "An application of a semi-hidden Markov model in wireless communication systems," *Mathematical Sciences*, vol. 13, no. 1, pp. 61–67, 2019.
- [10] D. G. Holmes, L. Cheng, M. Shimaponda-Nawa, A. D. Familua, and A. M. Abu-Mahfouz, "Modelling noise and pulse width modulation interference in indoor visible light communication channels," *AEU-International Journal of Electronics and Communications*, vol. 106, pp. 40–47, 2019.
- [11] G. Ndo, F. Labea, and M. Kassouf, "A Markov-Middleton model for bursty impulsive noise: Modeling and receiver design," *IEEE Transactions on Power Delivery*, vol. 28, no. 4, pp. 2317–2325, 2013.
- [12] A. D. Familua and L. Cheng, "First and second-order semi-hidden Fritchman Markov models for a multi-carrier based indoor narrowband power line communication system," *Physical Communication*, vol. 29, pp. 55–66, 2018.
- [13] J. Bilbao, A. Calvo, and I. Armendariz, "Fast characterization method and error sequence analysis for narrowband indoor powerline channel," in *17th International Symposium on Power Line Communications and Its Applications*, 2013, pp. 309–314.
- [14] V. Oksman and J. Zhang, "G.hnem: the new ITU-T standard on narrowband plc technology," *IEEE Communications Magazine*, vol. 49, no. 12, pp. 36–44, 2011.
- [15] M. Hoch, "Comparison of PLC G3 and PRIME," in *15th IEEE International Symposium on Power Line Communications and Its Applications*, 2011, pp. 165–169.
- [16] Ettus Research, *USRP N210*, (last accessed: May 8, 2020). [Online]. Available: <https://www.ettus.com/all-products/un210-kit/>
- [17] D. Sinha, A. K. Verma, and S. Kumar, "Software defined radio: Operation, challenges and possible solutions," in *10th International Conference on Intelligent Systems and Control (ISCO)*, 2016, pp. 1–5.
- [18] B. Fritchman, "A binary channel characterization using partitioned Markov chains," *IEEE Transactions on Information Theory*, vol. 13, no. 2, pp. 221–227, 1967.
- [19] W. H. Tranter, T. S. Rappaport, K. L. Kosbar, and K. S. Shanmugan, *Principles of Communication Systems Simulation with Wireless Applications*, 1st ed. Prentice Hall New Jersey, 2004.
- [20] A. D. Familua, K. Ogunyanda, T. G. Swart, H. C. Ferreira, R. Van Olst, and L. Cheng, "Narrowband PLC channel modeling using USRP and PSK modulations," in *18th IEEE International Symposium on Power Line Communications and Its Applications*, 2014, pp. 156–161.
- [21] X. Zhang and X. Zhang, "Error characterization of underwater acoustic channels based on the simple Fritchman model," in *IEEE International Conference on Signal Processing, Communications and Computing (ICSPCC)*, 2016, pp. 1–5.